Current Science International
Volume: 12 | Issue: 03| July – Sept.| 2023

EISSN:2706-7920 ISSN: 2077-4435
DOI: 10.36632/csi/2023.12.3.26
Journal homepage: www.curresweb.com
Pages: 375-387

Magnetic Resonance Diffusion, Spectroscopy and Susceptibility Imaging in Evaluation of Cerebellopontine Angle Masses

Sara M. Elnehrawy, Omar A. M. Hasanin, Mohamed A. ELTomy and Tamer M. Dawoud

Department of Radiodiagnosis, Faculty of Medicine, Tanta University, Egypt

Received: 10 June 2023 **Accepted:** 06 July 2023 **Published:** 20 July 2023

ABSTRACT

Background: The cerebellopontine angle (CPA) is a triangular subarachnoid space located within the posterior cranial fossa and centered at the level of the internal audiotary canal. Approximately 10%of intracranial tumors arise in the cerebellopontine angle and 80% of these are vestibular schwannomas**.** The majority of the remaining 20%are meningiomas, with rare incidance of facial or trigeminal schwannomas, epidermoid cysts(primarycholeseatomas), glomus jugular tumors, arachnoid cysts, giant cell tumors, metastatic deposits, and other masses. **Objective:** To evaluate the role of DWI, susceptibility and specrtroscopy in evaluation of cerebello pontine angle masses. **Patients and methods:** Our study included thirty cases with CPA masses that were subjected to advanced MRI techniques (DWI, SWi and, MRS) in addition to the conventional MRI techniques to evaluate their role in evaluation of CPA masses. **Results:** By using DWI in our protocol, we proved that; It can differentiate shwannomas, meningiomas and epidermoid cyst; where meningiomas are always restricted with low ADC values (mean ADC value < 1× 10−3 mm2 /s) while shwannomas have higher ADC values (mean ADC value >1× 10−3 mm2 /s) and epidermoid cysts are restricted with ADC values <1× 10−3 mm2 /s. By using SWI: SWI also proved to has an important value in differentiating meningiomas and shwannomas where in our study no meningiomas showed blooming on SWI while 61.5 % of shwannomas showed blooming (likely due to intra-lesional hemorrhage). Thus the presence of blooming within a lesion (after exclusion of calcifications) would rather the diagnosis of shwannoma than meningioma. By using MRS: 100% of shwannomas showed myo-inositol peak in our study and 87.5% of meningiomas showed alanine peak and 100% of meningiomas showed glutamate\glutamine peak, proving that MRS can be an accurate technique in differentiating the two entities. 100% of metastatic lesions showed choline peak in our study so MRS has an important value in the diagnosis of metastatic lesions. **Conclusion:** Advanced MRI techniques as DWI, susceptibility and spectroscopy have a great value in evaluation of CPA masses.

Keywords: cerebellopontine angle, intracranial tumors, susceptibility and specrtroscopy, cerebello pontine

1. Introduction

The cerebellopontine angle (CPA) is a triangular subarachnoid space located within the posterior cranial fossa and centered at the level of the internal audiotary canal. The apex of the space is medially positioned within the prepontine cistern, the petrous temporal bone forms the anterolateral border, and the cerebellum forms the posteromedial border. The space extends craniocaudally from the cranial nerve V to the cranial nerve IX_X_XI complex (Bonneville *et al.,* 2007; Smirniotopoulos *et al.,* 1993).

Approximately 10% of intracranial tumors arise in the cerebellopontine angle and 80% of these are vestibular schwannomas (Nikolopoulos *et al.,* 2010; Springborg *et al.,* 2008).

Corresponding Author: Sara Mostafa Elnehrawy, Department of Radiodiagnosis, Faculty of Medicine, Tanta University, Egypt.

The majority of the remaining 20%are meningiomas, with rare incidance of facial or trigeminal schwannomas, epidermoid cysts (primary choleseatomas), glomus jugular tumors, arachnoid cysts, giant cell tumors, metastatic deposits, and other masses (Moffat *et al.,* 1995).

Each of these masses requires specialized treatment and carries aunique prognostic profile Therefore, clinical differentiation between masses of the CPA is acritical for optimal treatment planning (Friedmann *et al.,* 2015).

CPA lesions clinically non-specific and the presenting symptoms are not related to the nature of the lesion itself, but to the nerves or cerebral structures involved with in the lesions, Cerebellopontine Angle masses may cause hearing loss, tinnitus and vertigo .Symptoms are typically of insidious onset , but sudden hearing loss or vertigo may occur ,facial numbness may be seen with large tumors due to compression of the trigeminal nerve .Facial nerve dysfunction from vestibular schwannoma is uncommon ;therefore, preoperative diagnosis of a CPA region tumor is mainly based on imaging. Diagnosis may be difficult because of the wide variety of cell types and origins of such tumors (De Foer *et al.,* 2014).

While surgical pathology is the diagnostic gold standard, clinical and radiologic features help to differentiate between CPA masses. Magnetic resonance imaging (MRI) is the most powerful noninvasive diagnostic tool for this purpose, and many CPA masses have distinct classic MRI features which may help with identification (Carlson *et al.,* 2012; Farid, 2014; Saloner *et al.,* 2010; Guermazi *et al.,* 2005).

Conventional MR imaging provides highly detailed anatomic information and has become amain in the diagnosis of suspicious brain lesions. Contrast -enhanced MR imaging has greatly improved the diagnostic accuracy of MR imaging (Moritani *et al.,* 2009).

Diffusion-weighted imaging (DWI) has been utilized for temporal bone and CPA imaging, particularly when abscesses or epidermoid/cholesteatoma are suspected. Diffusion restriction is seen with these pathologies and this specific sequence can be helpful in differentiation from other conditions (Turski *et al.,* 2016).

Vestibular schwannoma may sometimes be difficult to be differentiated from cerebellopontine angle meningiomas, demonstration of intra mural micro hemorrhgage with T2_susceptibility weighted imaging shows characteristic feature of identifying vestibular schwannomas from that of meningiomas (Radhakrishnan *et al.,* 2008).

Localized proton magnetic resonance spectroscopy (H_MRS) of the human brain is a mature methodology used clinically worldwide for evaluation of brain tumors. H-MRS may help with differential diagnosis, histlogic grading, degree of infiltration, tumor recurrence, and response to treatment, ainly when radiation necrosis develops and is indistinguishable from tumor by conventional magnetic resonance (MR) imaging (Brandao and Castillo, 2016).

The aim of this work is to evaluate additional diagnostic role of MRI diffusion and susceptibility imaging and MR spectroscopy in differentiation of cerebellopontine angle masses.

2. Patients and Methods

This study was carried out on 30 patients who suspected to have cerebellopontine angle masses after clinical examination by neurosurgeon at Neurosurgery department who were referred to radio-diagnosis and imaging department at Tanta University Hospital for MRI examination and evaluation. This study was performed at period from July 2020 to July 2021.

The age of patients ranged from 30 to 65 years (mean age 48.73 years). Informed consent was taken from patients.

Inclusion Criteria:

No gender predilection. Patient suspected to have cerebellopontine angle lesion by clinical examination or after CT scan examination.

Exclusion Criteria

Un-cooperative patient Patients with mental or behavioral disorder. Subjects with a contraindication to MRI as having any metallic implants as cochlear implants, metallic foreign bodies, or any other electronic or magnetically activated implants as well as claustrophobic patients.

Methodology:

All selected patients will be subjected to the following: History taking from patient or parents including: Patient's name, age and sex. History of the current illness; onset, course and duration of any complaints as headache, hearing loss. Family history of any CNS anomalies.

Imaging: MRI Evaluation:

Technique of Scanning: Magnetic resonance imaging was performed at closed 1.5 T MRI GE 1.5 (General Electric) machine using a standard imaging head coil.

Our examination included the following sequences: Conventional MRI sequences including: T2WI (axial across whole brain), T2WI (axial and coronal across CPA), T1WI pre-and post-contrast: axial and coronal across CPA and axial FLAIR across whole brain. MR advanced techniques including diffusion-weighted images (axial across whole brain), SWI and MR spectroscopy.

Each patient was administered 1 ml mol/kg of Gadolinium DPTA intravenously. Reconstruction was done using sophisticated workstation (general electric) including coronal, Sagittal oblique and MIP reformatting of the SSFP sequences.

The parameters of the different sequences were as follows: T2WI (TR 4045 ms, TE 110 ms, FOV 23x18.5 cm mm, Flip angle 90 °, Slice thickness 5 mm, and inter-slice gap 1mm). Thin cut T2WI (TR 3360 ms, TE 81 ms, FOV 17x15 cm, Flip angle 90°, Slice thickness 3 mm, and inter-slice gap 0.3 mm.). Thin cuts T1WI (TR 500 ms, TE 10 ms, FOV 17x15 cm, Flip angle 90°, Slice thickness 3 mm and inter-slice gap 0.3mm). FLAIR (TR 10000 ms, TE 140 ms, FOV 23x23 cm, Flip angle 90 °, Slice. thickness 5 mm Informed consent was taken from patients. DWI (TR 2095 ms, TE 90 ms, FOV 23X18.5 cm, Flip angle 90 °, Slice thickness 5 mm and inter-slice gap 1 mm).

The diffusion-sensitizing gradients were applied with a b factor of 0 and 1000 mm2/s per axis in each patient. The b-value used in this study has been determined by the specifications of the MR-scanner.

ADC maps were automatically reconstructed for all DW images and used for the measurement of ADC values in regions of interest (ROIs) at center of the lesions. The ADC values were expressed in × 10–3 mm2/s: SWI (TR 52 ms, TE 12 ms, FOV 23x23, Flip angle 20°, Slice thickness 5 mm and inter-slice gap 1 mm).

The acquisition time was 2 and half minutes approximately. Post processing was performed, followed by generation of thick minimum intensity projection (MIP) slabs.

The acquisition time was 3:30 minutes and the total scan time was 10 minutes. Multiplanar reconstruction was performed: MRS

In all cases, single-voxel 1H-MR spectroscopy was performed. A volume of interest (VOI) between 1cm³ and 8cm³ was placed on the lesion where the largest possible voxel was positioned within the enhancing part of the brain lesion with minimal contamination from the surrounding tissue.

Two spectra were acquired from the same VOI for every case at: 1. Short TE (2000/31) (TR/TE), 2. Long TE (2000/144).

Spectrum analysis was performed using software spectro within the MR scanner. The intensities of the data points of the spectrum between 0 and 4.00 ppm were selected and used as input for the normalization and statistical analysis. The resonances of interest were lipid at 1.30 ppm, lactate as an inverted doublet centered at 1.35 ppm, alanine at 1.47 ppm, N- acetyl-aspartate at 2.02 ppm, glutamate and glutamine at 2.35 ppm, creatine at 3.03 ppm, and choline and at 3.20 ppm. Special attention was paid to differentiation between lactate and alanine using the MRUI software II).

Image Analysis:

On conventional MRI sequence, the lesion was analyzed according to its signal intensity (hypo, iso, hyper-intense or bright), enhancing pattern (hyper, hypo or moderate/homogenous or heterogeneous), presence of cystic changes, its extension into and flaring of the IAC, the presence of dural tail, the presence extra-cranial extension. On DWI, the lesion was analyzed according to whether it was hyper, iso or hypo-intense and the ADC value was categorized to less than 1, from 1 to 1.7 and more than 1.8: Hyper-intense lesions with ADC value less than 1 are considered highly restricted. Hypo-intense lesions with ADC values more than 1.8 are considered non-restricted. Hyper and iso –intense lesions with ADC values between 1 and 1.7 are considered moderately restricted.

On SWI the lesions were analyzed according to the presence of intra-lesional signal voids that signify intra-lesional hemorrhage or calcifications.The finding were evaluated in filtered images to

differentiate between calcifications and hemorrhage. The filtered phase images were examined on the right _handed machine as follows: the hemorrhage appear low signal while calcification appear high signal. On MRS, the lesions were mainly analyzed according to the presence of different metabolites as alanine, myoinositol or choline peaks.

3. Results

As regarding the complain of our thirty patients; sixteen patients presented with sensorineural hearing loss; eight were diagnosed as vestibular shwannoma, six were diagnosed as meningioma and two were diagnosed as gliomas. Also ten patients presented with headache; four were diagnosed schwannoma, two were diagnosed as meningioma, one was diagnosed as epidermoid cyst, two were diagnosed as metastatic lesions and one was diagnosed as cystic epyndymoma. Four patients presented with tinnitus, one of them was diagnosed vestibular shwannomas, two were diagnosed as epidermoid cyst and one was metastasis (Table 1).

Table 1: Distribution of the studied cases according to the complaint (n = 30)

Complaint	Diagnosis									
	Schwannoma (n = 13)		Meningioma (n = 8)		Epidermoid cyst (n = 3)		Others (n = 6)		$\chi^{2\ MC}$	p
	No.	%	No.	%	No.	%	No.	%		
Sensory neural hearing loss	8	61.5	6	75.0	0	0.0	2	33.3	8.750	0.122
Headache	4	30.8	2	25.0	1	33.3	3	50.0		
Tinnitus	1	7.7	0	0.0	2	66.7	1	16.7		

χ^2: Chi square test MC: Monte Carlo p: p value for association between different categories *: Statistically significant at $p \leq 0.05$

As regarding the enhancement: 76.9% of schwannoma showed heterogenous enhancement and 23.1% showed marginal enhancement. 100% of meningioma showed homogenous enhancement .100% of epidermoid cysts showed no enhancement 100% of metastatic lesions and glioma showed heterogenous enhancement .100% of cystic ependymoma showed marginal enhancement (Table 2).

Table 2: Relation between diagnosis and signal intensity (n= 30) and enhancement

	Diagnosis								χ^2 MCp	
	Schwannoma (n = 13)		Meningioma (n = 8)		Epidermoid cyst (n = 3)		Others (n = 6)			
	No.	%	No.	%	No.	%	No.	%		
T1 (signal intensity)										
Hypo	6	46.2	0	0.0	3	100.0	1	16.7	10.822*	0.005*
ISO	7	53.8	8	100.0	0	0.0	5	83.3		
T2 (signal intensity)										
Hyper	3	23.1	8	100.0	3	100.0	1	16.7	17.336*	<0.001*
Heterogenous	10	76.9	0	0.0	0	0.0	5	83.3		
Enhancement										
Marginal	3	23.1	0	0.0	0	0.0	1	16.7	26.313*	<0.001*
Heterogenous	10	76.9	0	0.0	0	0.0	5	83.3		
Homogenous	0	0.0	8	100.0	0	0.0	0	0.0		
No enhancement	0	0.0	0	0.0	3	100.0				

χ^2: Chi square test MC: Monte Carlo p: p value for association between different categories *: Statistically significant at $p \leq 0.05$

As regarding DWI: 53.5% of schwannomas were (hyper dense) restricted in DWI, 38.5% were iso intense in DWI. In meningioma:100% of meningiomas were (hyper dense) restricted in DWI, also 100% of epidermoid cyst were restricted (hyper dense) in DWI. The metastatic lesions and gliomas were restricted in DWI while cystic ependymoma showed free diffusion (hypo dense) in DWI (Table 3).

Table 3: Relation between diagnosis and DWI (n = 30)

DWI	Diagnosis									
	Schwannoma (n = 13)		Meningioma (n = 8)		Epidermoid cyst (n = 3)		Others p (n = 6)		χ^{2MC}	
	No.	%	No.	%	No.	%	No.	%		
Hypo dense(free)	0	0.0	0	0.0	0	0.0	1	16.7	12.104	0.085
ISO	5	38.5	0	0.0	0	0.0	0	0.0		
High& hypo dense foci	1	7.7	0	0.0	0	0.0	0	0.0		
Hyper dense (restricted)	7	53.8	8	100.0	3	100.0	5	83.3		

χ^2: Chi square test MC: Monte Carlo p: p value for association between different categories *: Statistically significant at $p \leq 0.05$ H: H for Kruskal Wallis test p: p value for association between different categories.

As regarding MRS; All the eleven shwannomas (100%) showed myoinositol peak on MRS, seven meningiomas (85.7%) showed Alanine peak and one meningioma showed myoinositol peak (12.5%) ,100% of meningiomas showed glutamate\glutamine peak and the three metastatic lesions (100%) showed choline peak on MRS. In the other lesions it was difficult to get data from MRS curves due to the adjacent skull and bone artifact (Table 4).

Table 4: Relation between diagnosis and MRS (n = 22)

	Diagnosis							
	Schwannoma (n = 11)		Meningioma (n = 8)		Metastatic lesion (n = 3)		χ^2	p
	No.	%	No.	%	No.	%		
MRS								
Alanine peak	0	0.0	7	87.5	0	0.0		
Myoinositol peak	11	100.0	1	12.5	0	0.0	**27.341***	**^{MC}p <0.001***
Choline peak	0	0.0	0	0.0	3	100.0		
Glutamate/glutamine peak	0	0.0	8	100	0	0.0	**22.117***	**^{MC}p <0.001***

χ^2: Chi square test MC: Monte Carlo p: p value for association between different categories *: Statistically significant at $p \leq 0.05$

Case Presentation

Case 1: Male patient aged 45 years presented with headache.

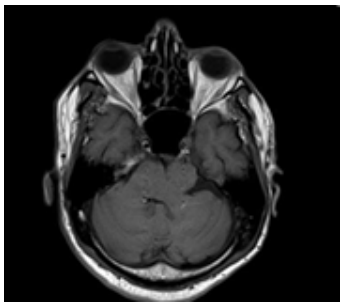

(A) Axial T1 pre-contrast

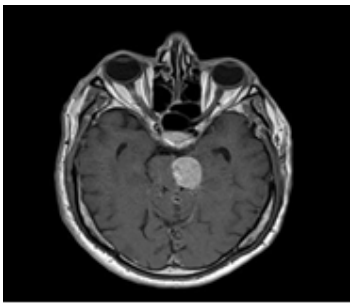

(B) Axial T1 post-contrast

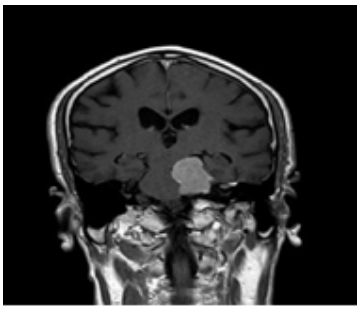

(C) Coronal T1 post-contrast

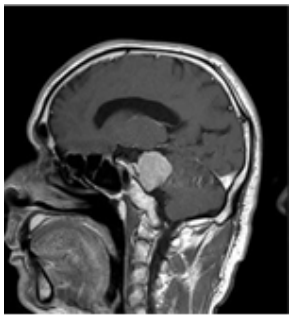

(D) Sagittal T1 post-contras

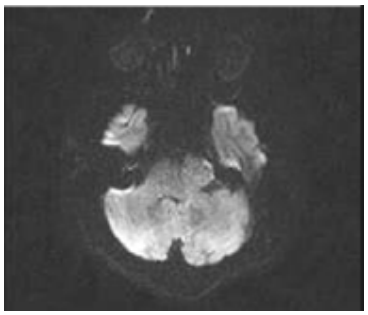

(E) DWI

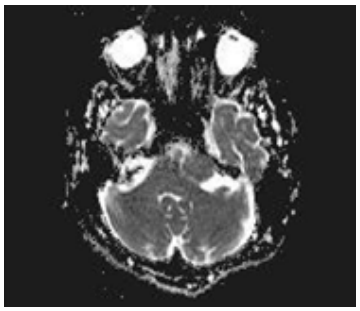

(F) ADC

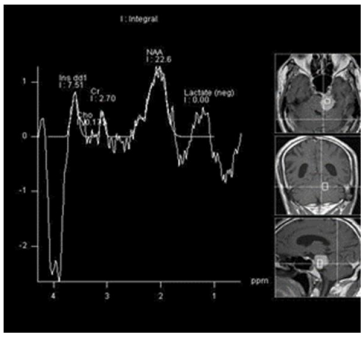

G) MRS

Left CPA space occupying lesion; seen iso-intense on T1WI (A), homogenous post-contrast enhacement (B, C, D), seen restricted on DWI (E), with ADC value 0.8× 10−3 mm2 (F) and showing Alanine peak on MRS (G).

These findings were matching with the final diagnosis of left CPA meningioma.

Case 2: 40 years old female presented with headache

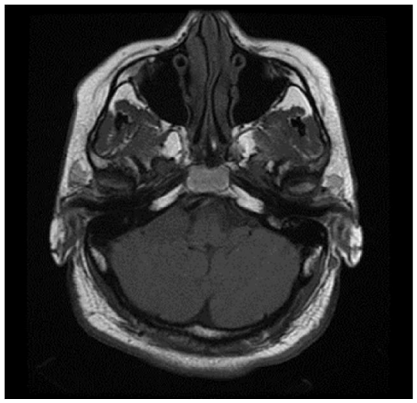

A) Axial T1WI

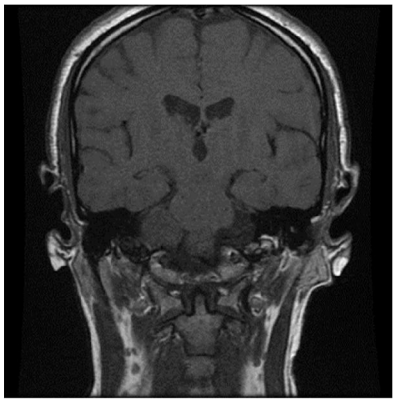

B) Coronal T1WI

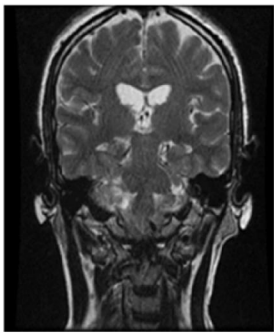

C) Coronal T2WI

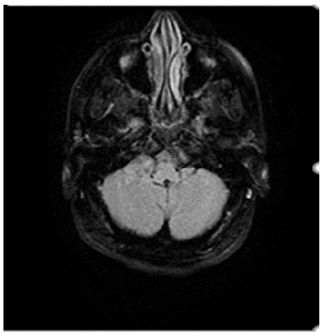

D) Axial T2WI flair

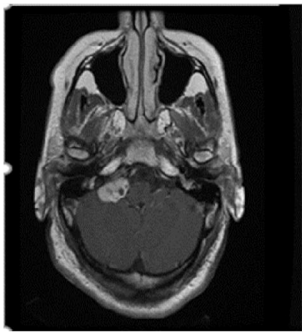

E) Axial T1WI post contrast

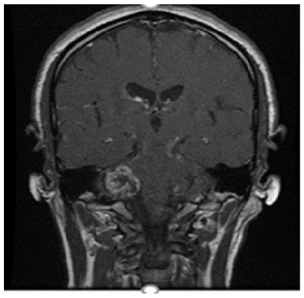

F) Coronal T1WI post-contrast

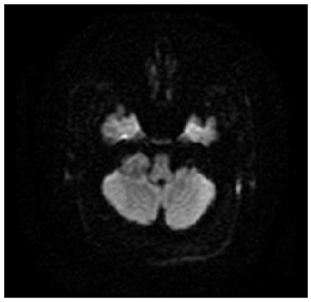

G) DWI

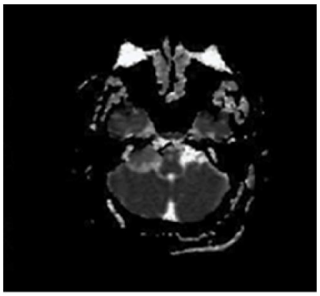

H) ADC

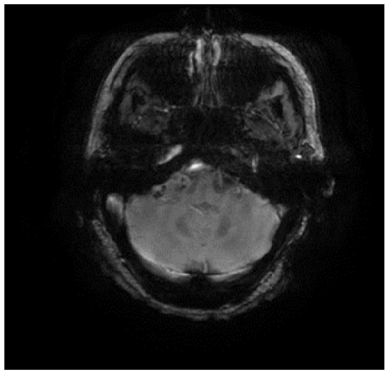

I) SWAN

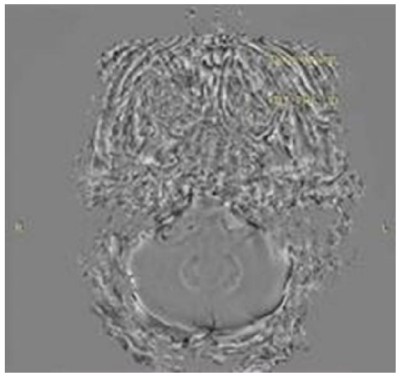

J) Filter

Well defined soft tissue lesion seen in the right cerebello-pontine angle showing intra canalecular extension. The lesion minimally indenting the right cerebello-pontine junction. The lesion

displays iso to hypo intense signal in T1WI (A, B) , high signal in T2WI and flair (C,D)), the lesion showing peripheral intense enhancement with central area devoid of contrast likely central degeneration (E,F), with restricted diffusion in DWI (G), with ADC value 1.25*10-3mm2/s (H), shows signal voids on SWAN (I) and show low signal dots on filter image (J) corresponding to heamorrahge. The final diagnosis is matching with right cerebllo-pontine of acoustic shwannoma.

Case 3: Male patient 30 years old presented with headache

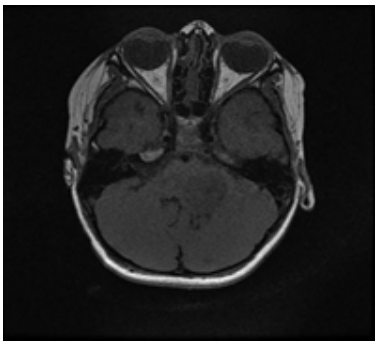

A) Axial T1WI

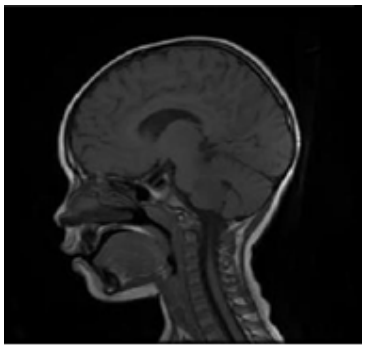

B) Sagittal T1WI

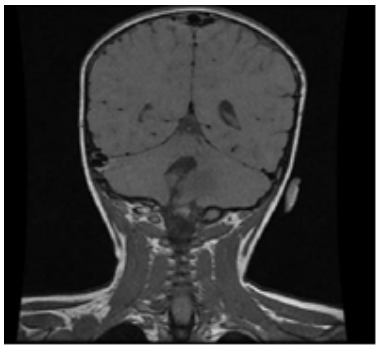

C)Coronal T1WI

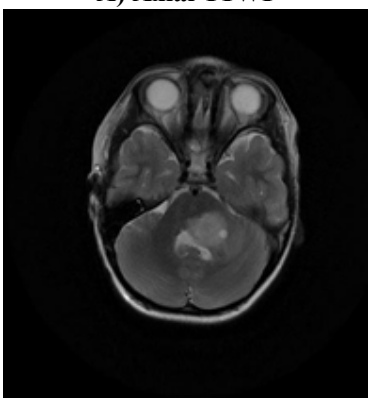

D) Axial T2WI

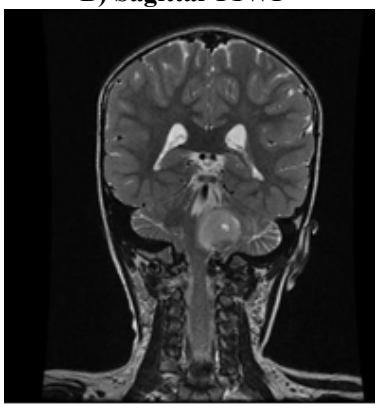

E) Coronal T2WI

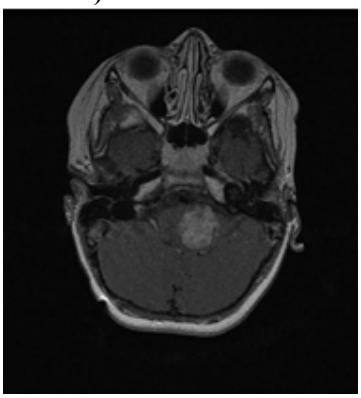

F) Axial T1WI post-contrast

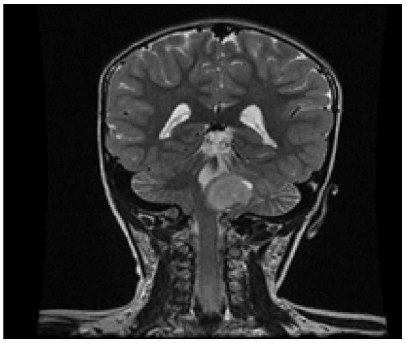

G) Coronal T2WI post -contrast

(H) Axial T2WI flair

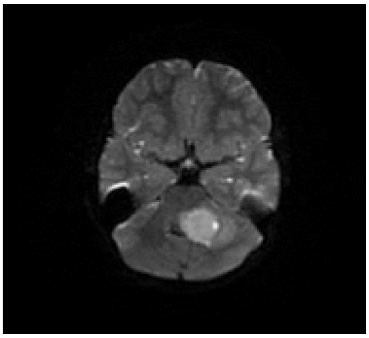

(I) DWI

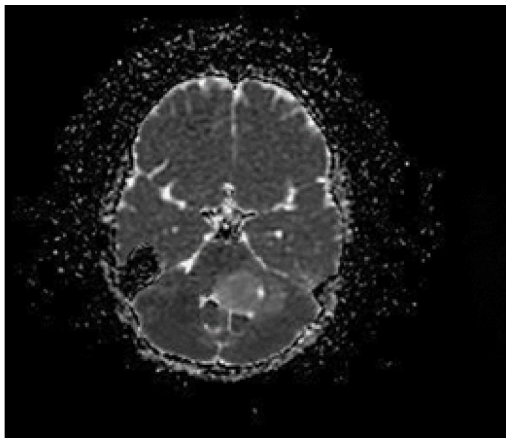

I) ADC

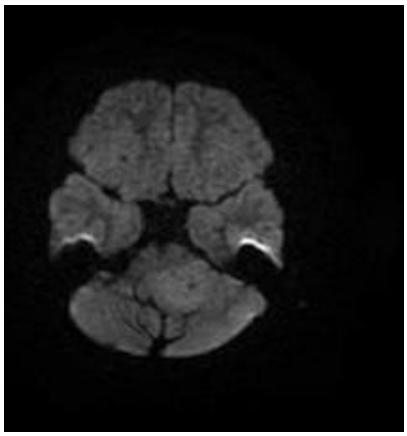

K) SWAN

A well-defined space occupying lesion seen occupying the posterior aspect of the pons extending into the CPA, which shows iso-intenisity in T1WI (A, B, C), shows heterogenous intenisity in T2WI (D, E) heterogenous enhancement in post contrast images and flair (F, G, H), and showed {T2 shine through} in DWI (I) with ADC value1.29 *10-3mm2\s (J), and show signal voids donating hemorrhage in SWAN (K) The finding is matching with lt brain stem glioma.

4. Discussion

At the early twentieth century, CPA lesions were difficult to diagnose and rarely completely excised with high mortality rate approaching about 50% (Alane and Gadre, 2004). However, recent techniques in neuroimaging and surgical techniques have made these lesions almost treatable with very low mortality rates (Mersha *et al.,* 2018).

CT and MRI are the main modalities for the diagnosis of cerebello-pontine angle masses (Yadav *et al.,* 2015). Although CT demonstrates the temporal bone and the osseous labyrinth, MRI is considered the imaging modality of choice for evaluation CPA masses due to itsexcellent soft tissue contrast, absence of beam-hardening artifacts and multi-planar imaging capability (Maaly and Sultan, 2016).

CPA masses can either be extra-axial or intra-axial. The presenting symptoms of CPA lesions are not related to the nature of the lesion itself but depend on the origin of the lesion and displacement of the neuro-vascular structures, thus they have no specific signs and symptoms (Maaly and Sultan, 2016).

Our study included thirty cases with CPA masses that were subjected to advanced MRI techniques (DWI, SWi and, MRS) in addition to the conventional MRI techniques to evaluate their role in evaluation of CPA masses.

In the present study, the masses occurred most frequently in the fourth and fifth decade representing 56.7 % of our cases; similar to patients reported by Sonowal *et al.* (2016) and Haque *et al.* (2011) who reported that the peak incidence of CPA masses to be in the fifth decade. Mersha *et al.* (2018), Singh *et al.* (2015) and. (Maaly and Sultan, 2016) reported the peak incidence of CPA tumors to be the third and fourth decade.

Our study agreed with Hari *et al.* (2016) who reported slight male preponderance but did not agree with Singh *et al.* (2015) who reported female predominance.

The most common presenting symptom in our study was sensory neural hearing loss (53.3%), followed by headache (33.3%) then tinnitus (13.3). This agreed with (Maaly and Sultan, 2016), Sonowal *et al.* (2016) who reported sensorineuralhearing loss as the most common presenting symptom in CPA masses.

In our study, acoustic shwannoma represented the most commonCPA lesion 36.7%), followed by meningioma (26.7%) then epidermoid(10%) This correlated well with most of the studies including (Maaly and Sultan, 2016), and Springborg *et al.* (2008) who reported that vestibular shwannomas meningiomas and epidermoid cysts are the three most common CPA lesions

respectively.

Our study included thirteen shwannomas; eleven vestibular shwannoma and two trigeminal shwannoma.

Vestibular shwannomas were the most common CPA lesion in our study. Their size ranged from 1 to 3.5 cm (40%: 2-2.5 cm, 35%: 1-1.5 cm, 25%: 3-3.5 cm). Eight acoustic shwannomas had acute angle with the IAC. Nine acoustic shwannomas had the classic "ice cream on cone" appearance and showed extension into the IAC. Ten (76.9%) were heterogenous after contrast administration.

Our study agreed with most of the studies regarding the enhancement pattern of acoustic shwannomas including Haque *et al.* (2011), Kapoor and Kulkarni, (2018) and (Maaly and Sultan, 2016) who reported acoustic shwannoma to show homogenous to heterogeneous enhancement in most of the cases.

On DWI, five (38.5%) shwannomas were iso-intense, seven (53.8%) were hyper-intense and one (10%) was hyper intense with hypodense foci (7.7%). All of shwannomas had ADC values more than 1.7× 10−3 mm2 /s.

In our study, all the 13 shwannomas had SWI done; eight (61.5%) of which showed signal voids and five (38.5) of which did not show signal voids. Saravanan *et al.* (2018) had SWI done on all their patients and reported that all the shwannoma cases in their study showed blooming on SWI that proved to be due to intra-lesional hemorrhagic foci after exclusion of calcifications by CT.

In our study, on MRS all shwannomas showed the characteristic myo-inositol peak at 3.55 ppm. This is Agree with Shakweer and Abdel Azim, (2015) reported that shwannomas showed myo-inositol peak.

Meningiomas were the second most common CPA lesion in our study. They were variable sized ranging from 1.5 to 4.5 cm. All of them were broad based and had obtuse angle with the IAC

In our study eight (100%) meningiomas were iso-intense on T1WI agreeing with most of the studies including Shakweer and Abdel Azim, (2015) who stated that meningiomas are mostly iso-intense on T1WI.

Eight (100%) meningiomas were hyper-intense on T2WI in our study. Mersha *et al.* (2018), reported 80% of their meningioma cases to be T2 hyper-intense on T2WI.

Eight (100%) meningiomas were homogenously hyper- enhancing with dural tail and no cystic changes agreeing with Shakweer and Abdel Azim, (2015) who stated that 100% of their meningioma cases showed intense homogenous enhancement.

In our study, all the eight (100%) meningiomas were hyper-intense on DWI. With ADC values less than 1× 10−3 mm2/s. SWI was done all cases of meningiomas in our study; none of which showed signal voids agreeing with Saravanan *et al.* (2018) who had SWI done on all their patients and reported that no meningiomas showed blooming

On MR spectroscopy; seven cases (87.5%) showed Alanine peak in our study. One case (12.5) showed myoinositol peak None showed glutamine peak or high choline/ creatine, agreeing with Kinoshita and Yokota, (1997) who stated that meningiomas showed thecharacteristic alanine peak at 1.5 ppm and didn‟ t show high choline peak.

Epidermoids are the third most common CPA lesions. Our study included 3 epidermoids. In our study, the three epidermoids (100%) were hypo-intense on T1WI, hyper intense on T2WI and showed no enhancement after contrast administration.

On DWI, the epidermoids (100%) were hyper-intense with mean ADC value more than 1.1× 10−3 mm2 /s and did not show signal voids in SWI. These findings agreed with Hasegawa *et al.* (2016), and Farhan and Abdulsttar, (2018) who stated that epidermoids and arachnoid cysts are T1 hypo-intense, T2 hyper-intense and that both of them show no post contrast enhancement. They also stated that epidermoids show restricted diffusion while arachnoid cysts don't restrict.

Our study included three metastatic lesions. They were known leukemic patients that came for follow up to exclude cranial metastasis, the three metastasis were iso- intense in T1WI, heterogenous intensity in T2WI and show heterogenous enhancement after contrast administration.

On DWI, the metastasis was hyper intense with ADC value more than 1.1× 10−3 mm2 /s and showed signal voids in SWI.

On MRS, the metastasis showed choline peak, which agreed with Danieslen and Ross, (1999) who stated that Choline (Cho) is seen as a peak at 3.2 ppm.

Our study included two gliomas, they were iso-intense in T1WI, heterogenous intenisity in T2WI and show heterogenous enhancement after contrast administration.

These findings agreed with Guillamo *et al.* (2001), who stated that adult brain stem gliomas mainly affect the pons in 64% of patients, followed by the medulla in 51% and the midbrain in 43% and appear hypo intense in T1WI, hyper intense at T2WI, showed heterogenous or marginal enhancement after contrast administration.

Our study included one cystic ependymoma. It was hypo-intense in T1WI, hyper –intense in T2WI and showed marginal enhancement after contrast administration.

On DWI,cystic ependymoma showed free diffusion with ADC value 2.5× 10−3 mm2 /s and showed no signal voids in SWI.

These findings agreed with Yang *et al.* (2014) who stated that CPA ependymoma mostly appear lobulated or multilobulated in the posterior fossa and are hypointense in TIWI ,hyper intense in T2WI and heterogenous after contrast administration mainly due to hemorrhage,cystic changes and necroris.

4. Conclusions

In the present study, we found that the advanced MRI techniques are of great value to differentiate and to reach the accurate diagnosis of different CPA masses.

DWI: By using DWI in our protocol, we proved that; It can differentiate shwannomas, meningiomas and epidermoid cyst; where meningiomas are always restricted with low ADC values (mean ADC value< 1× 10−3 mm2 /s) while shwannomas have higher ADC values (mean ADC value >1× 10−3 mm2 /s) and epidermoid cysts are restricted with ADC values <1× 10−3 mm2 /s.

SWI: SWI also proved to has an important value in differentiating meningiomas and shwannomas where in our study no meningioms showed blooming on SWI while 61.5 % of shwannomas showed blooming (likely due to intra lesional hemorrhage). Thus the presence of blooming within a lesion (after exclusion of calcifications) would rather the diagnosis of shwannoma than meningioma.

MRS: 100% of shwannomas showed myo-inositol peak in our study , 87.5% of meningiomas showed alanine peak and 100% of meningiomas showed glutamate\glutamine peak, proving that MRS can be an accurate technique in differentiating the two entities. 100% of metastatic lesions showed choline peak in our study so MRS has an important value in the diagnosis of metastatic lesions. MRI is the study of choice for characterization of CPA masses. Conventional MRI imagining can sometimes be sufficient to reach an accurate diagnosis. However, there are difficult cases where MR advanced techniques can give much more information regarding the lesion.

DWI differentiates highly cellular lesions such as meningiomas, epidermoids and metastasis from other less cellular lesions. On DWI, meningiomas are restricted with mean ADC value < 1× 10−3 mm2/s but shwannomas usually show intermediate restriction with mean ADC value > 1 × 10−3 mm2/s.

On SWI shwannomas usually show intra-lesional signal voids representing foci of micro-hemorrhages but when meningioma shows signal voids, they represent intra-lesional calcifications which can be proved by the filtered phase image or CT. MR spectroscopy differentiates different lesions according to the metabolites found within them, such as the presence of myoinositol within shwannomas and alanine within meningiomas.

References

Alane, L.C., and A. Gadre, 2004. Presentation UT MB Dept. of Otolaryngology. University Texas, Medical Branch 2004

Bonneville, F., J. Savatovky and J. Chiras, 2007. Imaging of cerebello pontine angle masses: an update. Part1: enhancing extra-axial lesions. EurRadiol., 17(10):2472-2482.

Brandao L., and M. Castillo, 2016. Adult Brain Tumors: Clinical Applications of Magnetic Resonance Spectroscopy. Magnetic Resonance Imaging Clinics of North America, 24(4):781-809. DOI:10.1016/j.mric.2016.07.005

Carlson, M.L., K.M. Van Abel, C.L. Driscoll, 2012. Magnetic resonance imaging surveillance following vestibular schwannoma resection.Laryngoscope 2012; 122:378–88.

Danieslen E.R. and B. Ross, 1999. Magnetic resonance spectroscopy diagnosis of neurological disease. New York, Marcel Dekker, Inc.

De Foer, B., K. Carpentier, A. Bernaerts, 2014. Imaging of Cerebellopontine Angle and Internal Audiotary Canal Lesions, Temporal Bone Imaging Medical Radiology, Diagnostic ImagingDOl:10.1007\174-2014-1030.

Farhan, D.A. and O.A. Abdulsttar, 2018. Role of Diffusion-Weighted Image in Differentiation between Epidermoid Cyst and other Cerebellopontine Angle Masses. Med J Babylon, 15(3):238-42.

Farid, N., 2014. Imaging of vestibular schwannoma and other cerebellopontine angle tumors. Oper Tech Otolaryngol Head Neck Surg., 25:87– 95.

Friedmann, D.R., B. Grobelny, J.G. Golfinos, 2015. Nonschwannoma tumors of the cerebellopontine angle. Otolaryngol Clin North Am., 48:461–75.

Guermazi, A., F. Lafitte, Y. Miaux, 2005. The dural tail sign–beyond meningioma. Clin Radiol., 60:171–88.

Guillamo, J.S., F. Doz and J.Y. Delattre, 2001. Brainstem gliomas. CurrOpin Neural 14:711-715.

Haque, S., A. Hossain, M. Quddus, M. Jahan, 2011. Role of MRI in the evaluation of acoustic schwannoma and its comparison to histopathological findings. Bangladesh Med Res Counc Bull., 37(3):92-6.

Hari, P.S., J.A. Jyothi, M. Thatipamula, 2016. Study of posterior fossa tumors by high resolution MRI. J Evid Based Med Health, 3(6):197- 203.

Hasegawa, M., M. Nouri, S. Nagahisa, K. Yoshida, K. Adachi, J. Inamasu, et al., 2016. Cerebellopontine angle epidermoid cysts: clinical presentations and surgical outcome. Neurosurg Rev., 39(2):259- 67.

Kapoor, S. and V. Kulkarni, 2018. Role of MRI in Evaluation of Cerebello pontine angle tumour. J Adv Med Dent Scie Res., 6(9):15-8.

Kinoshita, Y. and A. Yokota, 1997. Absolute concentrations of metabolites in human brain tumors using in vitro proton magnetic resonance spectroscopy. NMR Biomed 1997; 10(1):2-12.

Maaly, M.A. and A A. Sultan, 2016. Current role of MRI in cerebellopontine angle lesions. Menoufia Med J., 29(1):147.

Mersha, H., T. Kebebew and T. Debebe, 2018. Cerebellopontine angle masses: Radiologic-pathology correlation at tikur anbessa specialized hospital and myungsung christian medical center. Ethiop Med J 2018; 56(1):37-42.

Moffat, D.A. and R.H. Ballagh, 1995. Rare tumours of the cerebellopontine angle. Clin Oncol (R Coll Radiol), 7:28–41.

Moritani, T., S. Ekholom, P. Westesson, 2009. Diffusion_ Weighted MRImaging of the Brain .textbook2 (9)142_150.

Nikolopoulos, T.P., H. Fortnum, G. O'Donoghue, 2010. Acoustic neuroma growth: a systematic review of the evidence. Otol Neurotol., 31:478-85.

Radhakrishnan, K., 2008. Intramural micro hemorrhage on T2 Weighted Gradient- Echo Imaging Helps Differentiate Vestibular Schwannoma from Meningioma, AJNR Am. J. Neuroradiol Mar 2008; 29(3):552_570.

Saloner, D., A. Uzelac, S. Hetts, 2010. Modern meningioma imaging techniques. J. Neurooncol., 99:333–40.

Saravanan, K., E.A. Parthasarathy, A.S. Farook, P. Sridharan, R. Anand, 2018. Role of Susceptibility Weighted Imaging in Cerebellopontine Angle Schwannoma Vs Meningioma. Int J Contemp Med Sur Radiol 2018; 3(2):20-3.

Shakweer, M.M. and M.H. Abdel Azim, 2015. Differentiation between the common cerebellopontine angle (CPA) lesions by the new MRI techniques. Al-Azhar Assiut Med J., 13(1):1-17.

Singh, K., M.P. Singh, C. Thukral, K. Rao, K. Singh, A. Singh, 2015. Role of magnetic resonance imaging in evaluation of cerebellopontine angle schwannomas. Indian J Otolaryngol Head Neck Surg., 67(1):21- 7.

Smirniotopoulos, J.G., N.C. Yue and E.J. Rushing, 1993. Cerebellopontine angle masses: radiologic-pathologic correlation. Radiographics, 13 (5):1131-1147.

Sonowal, T.N., S. Agarwal, H. Choudhury, N. Brahma, 2016. Cerebellopontine angle lesions-ct and mr imaging evaluation. J Evol Med Dent Sci 2016; 5(91):6750-6.

Springborg, J.B., L. Poulsgaard and J. Thomsen, 2008. Nonvestibular schwannoma tumors in the cerebellopontine angle: a structured approach and management guidelines. Skull Base, 18:217–27.

Turski, P.S.A., E. Hartman, Z. Clark, 2016. Neurovascular 4DFlow MRI (Phase Contrast MRA): emerging clinical applications. Neurovascular Imaging, 2(8).

Yadav, P., M, Jantre and D. Thakkar, 2015. Magnetic resonance imaging of cerebellopontine angle lesions. Med J DY Patil Univ., 2015; 8(6):751-9.

Yang, X., Y. Ren, W. Wu, et al., 2014. Intra cranial extra axial ependymoma involving the petroclival region:Int J Clin EXP Pathol., 7:9076